

# Synchronization phenomena in multimode dynamics of coupled nephrons

*O.V. Sosnovtseva, A.N. Pavlov, E. Mosekilde, N.-H. Holstein-Rathlou*

The individual functional unit of the kidney (the nephron) displays oscillations in its regulation of the incoming blood flow at two different time scales: fast oscillations associated with a myogenic dynamics of the afferent arteriole, and slower oscillations arising from a delay in the tubuloglomerular feedback. The paper investigates the intra- and inter-nephron interactions of these two modes. Besides full synchronization, both wavelet analyses of experimental data and numerical simulations of a detailed physiological model reveal the occurrence of a partial entrainment in which neighboring nephrons attain a state of synchronization with respect to their slow dynamics, but the fast dynamics remain desynchronized.

## Introduction

The concept of homeostasis [1], i.e. the ability of the body to maintain a nearly constant internal milieu despite changes in the external conditions, plays an essential role in the description of physiological control systems. It is sometimes assumed that homeostasis implies that the physiological variables are kept near a stable steady state by means of effective feedback regulation. While this may be the case in certain situations, biological systems in general should be considered as open dissipative systems that are maintained under far-from-equilibrium conditions [2]. Regular and irregular oscillations associated with various forms of instability are common features of behavior that can be observed during normal functioning or arise in connection with particular states of disease [3].

The kidneys play an important role in regulating the blood pressure and maintaining a proper environment for the cells of the body. It is well-established that renal autoregulation is mediated by at least two mechanisms, the tubuloglomerular feedback (TGF) and the myogenic response of the afferent arteriole [4]. The TGF mechanism produces a negative feedback control that regulates the nephronal blood flow and, hence, the single-nephron glomerular filtration rate and the tubular flow rate in dependence of the NaCl concentration of the fluid that leaves the nephron. Experiments by Leyssac and Holstein-Rathlou [5, 6] have demonstrated that this feedback regulation can become unstable and generate self-sustained oscillations in the proximal intratubular pressure with a typical period of 30-40s. With different amplitudes and phases the same oscillations are manifest in the distal intratubular pressure and in the chloride concentration near the terminal part of the loop of Henle [7]. While for normal rats the oscillations have the appearance of a limit cycle with a sharply peaked power spectrum (Fig.1a), highly irregular oscillations are observed for spontaneously hypertensive rats (Fig.1b) [5].

The myogenic mechanism represents the intrinsic response of the smooth muscle cells in the the vascular wall to changes in the TGF-signal as well as to other stimuli. This mechanism operates at 0.1-0.2Hz. An increase of the transmural pressure elicits a contraction of the vascular smooth muscle causing a vasoconstriction and an increase in the resistance of the afferent arteriole. Since both mechanisms act on the afferent arteriole to control its hemodynamic resistance, the activation of one of the mechanisms modifies the response of the other [4].

Different forms of entrainment between the tubular pressure variations in adjacent nephrons were described in a couple of recent publications [8, 9]. Observation of both in-phase and anti-phase synchronization was reported for the regular pressure oscillations in normal rats while spontaneously hypertensive rats revealed signs of chaotic phase synchronization.

Entrainment phenomena are of considerable interest from a physiological point of view. It is known, for instance, that epileptic seizures are related with the synchronization of larger groups of cells in the brain [10]. In their normal physiological states, waves of cytoplasmic calcium are known to propagate across cell assemblies such as, for instance, smooth muscle cells and  $\beta$ -cells. For the kidney, the aggregate response of the ensemble of nephrons is expected to depend on their state of synchronization. While entrainment of single-mode deterministic or stochastic oscillations is well understood, the dynamics of systems with several oscillatory modes is less studied. Living systems often exhibit oscillations with different time scales. The thalamocortical relay neurons, for instance, can generate either spindle or delta oscillations [11]. It was recently found [12] that the electroreceptors in paddlefish can be biperiodic. In the present paper we describe the individual nephron as a two-mode oscillator demonstrating relatively fast oscillations associated with the myogenic regulation of the arteriolar diameter and slower oscillations related with the delay in the tubuloglomerular feedback. We study numerically as well as experimentally the entrainment between these time scales both within the individual nephron and between neighboring nephrons. We apply the wavelet-based techniques to describe features of entrainment in nonstationary dynamics of coupled nephrons.

## 1. Nephron Autoregulation

**1.1. Mathematical model.** Over the years significant efforts have been made to develop mathematical models that can account for the observed regular and irregular pressure variations and describe the physiological processes that occur along the tubular system [13, 14]. A particular aspect of this research has been to show that the transition from regular oscillations to irregular variations in the tubular pressure can be explained in terms of parameter changes within the framework of well-established physiological mechanisms. A review of the work may be found in the recent contribution by Andersen et al. [15]. Here, a model of nephron-nephron interaction was developed and it was shown that this model can produce a variety of different synchronization phenomena.

Autoregulation of the pressures and flows in the individual nephron may be described by the following model [14]:

$$\begin{aligned}
 \dot{P}_t &= \frac{1}{C_{tub}} \{F_f(P_t, r) - F_{reab} - (P_t - P_d)/R_H\}, \\
 \dot{r} &= v_r, \\
 \dot{v}_r &= \frac{1}{\omega} \{P_{av}(P_t, r) - P_{eq}(r, \Psi(X_3, \alpha), T) - \omega d v_r\}, \\
 \dot{X}_1 &= \frac{1}{R_H} (P_t - P_d) - \frac{3}{T} X_1, \\
 \dot{X}_2 &= \frac{3}{T} (X_1 - X_2), \\
 \dot{X}_3 &= \frac{3}{T} (X_2 - X_3).
 \end{aligned} \tag{1}$$

The first equation represents the pressure variations in the proximal tubule in terms of the in- and outgoing fluid flows. Here,  $F_f$  is the single-nephron glomerular filtration rate and  $C_{tub}$  is the elastic compliance of the tubule. The flow into the loop of Henle is determined by the difference  $(P_t - P_d)$  between the proximal and the distal tubular pressures and by the flow resistance  $R_H$ . The reabsorption in the proximal tubule  $F_{reab}$  is assumed to be constant.

The following two equations describe the dynamics associated with the flow control in the afferent arteriole. Here,  $r$  represents the radius of the active part of the vessel and  $v_r$  is its rate of increase.  $d$  is a characteristic time constant describing the damping of the oscillations,  $\omega$  is a measure of the mass relative to the elastic compliance of the arteriolar wall, and  $P_{av}$  denotes the average pressure in the active part of the arteriole.  $P_{eq}$  is the value of this pressure for which the arteriole is in equilibrium with its present radius and muscular activation  $\Psi$ . The expressions for  $F_f$ ,  $P_{av}$  and  $P_{eq}$  involve a number of algebraic equations that must be solved along with the integration of Eq.(1).

The remaining equations in the single-nephron model describe the delay  $T$  in the TGF regulation. This delay arises both from the transit time through the loop of Henle and from the cascaded enzymatic processes between the macula densa cells and the smooth muscle cells that control the contractions of the afferent arteriole. The feedback delay, which typically assumes a value of 12-18sec, will be considered a bifurcation parameter in our analysis. Another important parameter is the strength  $\alpha$  of the feedback regulation. This parameter takes a value of about 12 for normotensive rats, increasing to about 18 for hypertensive rats [16]. For a more detailed explanation of the model and the parameters, see Ref. [15].

Considering the model equations (1) we can identify the two time scales in terms of (i) a low-frequency (TGF-mediated) oscillation with a period  $T_h \cong 2.2T$  arising from the delay in the tubuloglomerular feedback, and (ii) somewhat faster oscillations with a period  $T_v \approx T_h/5$  associated with the inherent myogenic adjustment.

To determine  $T_h$  and  $T_v$  in our numerical simulations we have used the mean return times of the trajectory to appropriately chosen Poincaré sections

$$T_v = \langle T_{ret} \Big|_{\dot{v}_r=0} \rangle, \quad T_h = \langle T_{ret} \Big|_{\dot{X}_2=0} \rangle. \quad (2)$$

Here,  $T_{ret} \Big|_{\dot{v}_r=0}$  denotes the time between two subsequent crossings (from the same side) of the trajectory through the plane  $\dot{v}_r=0$ .

From these return times it is easy to calculate the intra-nephron rotation number (i.e., the rotation number associated with the two-mode behavior of the individual nephron)

$$r_{vh} = T_v/T_h. \quad (3)$$

With varying feedback delay  $T$  and varying slope  $\alpha$  of the open loop feedback curve, Fig.2 shows how the two oscillatory modes can adjust their dynamics and attain states with different rational relations ( $n : m$ ) between the periods. The regions of high resonances (1 : 4, 1 : 5, and 1 : 6) are seen to exist in the physiologically interesting range of the delay time  $T \in [12 \text{ sec}, 20 \text{ sec}]$ . However, some of these regions are relatively small, and there are neighboring regions with 2 : 11, 2 : 13, and chaotic dynamics. While the transitions between the different locking regimes always involve bifurcations, bifurcations may also occur within the individual regime. A period-doubling transition, for instance, does not necessarily change  $r_{vh}$ , and the intra-nephron rotation number may remain constant through a complete period-doubling cascade and into the chaotic regime [9].

**1.2. Experimental data analysis.** Physiological signals are generated by complex, self-regulating systems and may be extremely inhomogeneous and nonstationary. Processing of data series of this type by means of conventional techniques such as correlation and/or Fourier analysis can lead to misinterpretations of the results. That is why special techniques based on wavelet analysis become of a high interest [17]. Wavelets provide us with the possibility of

searching hidden periodicities in short, nonstationary data and follow the temporal evolution of different rhythmic components in the case of noisy multimode dynamics.

The wavelet transform of a signal  $x(u)$  can be written as:

$$T_x(a, t) = \frac{1}{\sqrt{a}} \int_{-\infty}^{\infty} x(u) \psi^* \left( \frac{u-t}{a} \right) du. \quad (4)$$

Here  $\psi$  is a “mother” function that in general can have an arbitrary shape provided it is soliton-like with zero average.  $T_x(a, t)$  are the wavelet coefficients,  $a$  being a time scaling and  $t$  a time displacement parameter. To investigate the presence of various rhythmic components, the *Morlet* wavelet is particularly useful. The given function consists of two terms, however, in practice one of them is small enough and can be ignored. One typically uses the following simplified expression for the Morlet function:

$$\psi(\tau) = \pi^{-1/4} \exp(-j2\pi k_0 \tau) \exp \left[ -\frac{\tau^2}{2} \right]. \quad (5)$$

This wavelet represents a harmonic oscillation with frequency  $f = k_0/a$  and with an amplitude that is modified in time by Gaussian factor describing how the wave arises and decays. For the frequency range being of interest in the dynamics of nephrons we can take  $k_0 = 1^1$ . In such a case the frequency  $f$  is the simple inversion of time scale  $a$ , and the expression for the wavelet transform can be rewritten as follows:

$$T_x(f, t) = \sqrt{f} \int_{-\infty}^{\infty} x(u) \psi^*(\tau) du, \quad \tau = f(u - t). \quad (6)$$

The wavelet transform  $T_x(f, t)$  measures the spectral contribution near the frequency  $f$  at time  $t$  of the observed signal.

Some authors [18] prefer to consider other complex wavelet functions because of possible spurious effects (especially for time series with nonzero mean). To avoid such problems we have transformed all time series to zero mean value before applying the wavelet technique.

In addition to the wavelet transform coefficients  $T_x(f, t)$  we can estimate the energy density  $E_x(f, t) = |T_x(f, t)|^2$ . As the result there is a surface in a 3-dimensional space  $E_x(f, t)$ . Sections of this surface at fixed time moments  $t = t_0$  correspond to the local energy spectrum. To simplify the visualization of the two-dimensional spectrum  $E_x(f, t)$  we can consider only the dynamics of the local maxima of  $E_x(f, t_0)$ , i.e., the peaks of the local spectra.

Figure 3 shows the different components detected in the time series of Fig.1. (Here, aiming to illustrate the complex nonstationary dynamics of real nephrons, we demonstrate all maxima of  $E_x(f, t_0)$  independently of their magnitudes). Inspection of the figure reveals that the slow oscillations, whether they are periodic or chaotic, maintain a nearly constant frequency through the observation time. The fast oscillations, on the other hand, fluctuate significantly, particularly for the hypertensive rat. This may be related to a complex modulation of the fast oscillations by the slow dynamics or to the influence of noise (since the fast oscillations are small in amplitude, they are more sensitive to fluctuations).

The presentation in Figure 3 does not provide information about the dominant spectral components. This information can be obtained, for example, from a so-called *scalogram*, i.e., a time averaged power spectrum, being an analogue to the Fourier power spectrum. Such a scalogram is illustrated in Fig. 4 where a well-pronounced peak around  $0.03Hz$ , corresponding to the slow TGF-mediated mode, is distinguishable. The other peak at  $0.15 - 0.2Hz$  derives

---

<sup>1</sup>The value  $k_0$  allows to search some compromise between localization of the wavelet function in both, time domain and frequency domain.

from the fast myogenic dynamics. It is interesting to note how clearly these oscillations can be detected from the tubular pressure variations. Since both the above frequency components are of physiological interest we extract them from the original wavelet transformation for further analysis of their coherence properties. Figure 5 displays the relation between fast and slow oscillations in a single nephron. For the periodic oscillations observed for normotensive rats (Fig.5a), the fast and slow components adjust their periods in accordance to one another to maintain a 1 : 5 entrainment during the observation time. For the chaotic oscillations observed for hypertensive rats (Fig.5b), the ratio changes more randomly in time.

We conclude that besides being regular or chaotic, the self-sustained pressure variations in the individual nephron can be classified as being synchronous or asynchronous with respect to the ratio between the two time scales that characterize the fast (arteriolar) mode and the slow (TGF mediated) mode, respectively. As we shall see, this complexity in behavior may play an essential role in the synchronization between a pair of interacting nephrons.

## 2. Entrainment of oscillatory modes for interacting nephrons

**2.1. Simulation results.** Neighboring nephrons can influence each other's blood supply either through vascularly propagated electrical (or electrochemical) signals or through a hemodynamic coupling arising via a direct redistribution of the blood flow between the coupled nephrons. While the hemodynamic coupling depends mainly on the flow resistances in the arteriolar network, the vascularly propagated coupling is associated with signal transmission between smooth muscle cells. The result is that only nephrons situated close to one another can interact via the vascularly propagated coupling. Nephrons situated farther apart but sharing a common piece of interlobular artery may interact via the hemodynamic coupling.

In the present work we shall focus our attention on the vascularly propagated coupling, assuming the hemodynamic coupling to be negligible. In the single-nephron model the equilibrium pressure in the afferent arteriole depends on the current radius  $r$  and on the activation level  $\Psi$  of the smooth muscles surrounding the arteriole and controlling its diameter. The muscular activation arises at the juxtaglomerular apparatus and travels upstream along the afferent arteriole in a damped fashion. When it reaches the branching point with the arteriole from the neighboring nephron, part of the signal may propagate down that arteriole and start to contribute to its TGF response. The coupling is considered nearly instantaneous since the time it takes for the vascular signal to reach the other nephron is very small relative to the period of the TGF-oscillations. It has been observed [19] that the signal decreases nearly exponentially as it propagates. Thus only a fraction,  $\gamma = e^{-l/l_0} < 1$ , of the original activation level reaches the vascular smooth muscles close to macula densa of the neighboring nephron. In the expression for the vascular coupling parameter  $\gamma$ ,  $l$  is the propagation length of the coupling signal, and  $l_0 \cong 500 \mu m$  is the characteristic length scale of the exponential decay. In the model, the vascularly propagated coupling is represented by adding a contribution of the activation level in one nephron to the activation level in the neighboring nephron:

$$\Psi_{1,2}^* = \Psi_{1,2} + \gamma\Psi_{2,1} \quad (7)$$

with  $\gamma$  being the coupling parameter and  $\Psi_{1,2}$  the uncoupled activation levels of the two nephrons as determined by their respective Henle flows. In view of the characteristic propagation length for the signal and of measured distances between neighboring nephrons along the arteriolar network, a typical value of  $\gamma$  is considered to be 0.1 - 0.2 [19]. By virtue of the two-mode dynamics of the individual nephron, a number of new and interesting results appear.

The individual oscillatory system has two modes that can be locked with each other. However, an interaction between functional units can break their mutual adjustment. It is also plausible that a coupling can act in different manners on the fast and slow oscillations. For the interacting systems we introduce two rotation numbers as follows:

$$r_v = T_{v1}/T_{v2}, \quad r_h = T_{h1}/T_{h2}. \quad (8)$$

To provide more information, the variation of the phase difference is calculated separately for the slow  $h$  and for the fast  $v$  oscillations.

Let us consider the case of  $\alpha = 30.0$  corresponding to a weakly developed chaotic attractor in the individual nephron. The coupling strength  $\gamma$  and delay time  $T_2$  in the second nephron are varied. Two different chaotic states can be recognized as asynchronous and synchronous (Fig.6). For asynchronous behavior the rotation numbers  $r_h$  and  $r_v$  change continuously with  $T_2$  while inside the synchronization region two cases can be distinguished. To the left, the rotation numbers  $r_h$  and  $r_v$  are both equal to unity since both slow and fast oscillations are synchronized. To the right ( $T_2 > 14.2 \text{ sec}$ ), while the slow  $h$ -mode of the chaotic oscillations remain locked, the fast  $v$ -mode drifts randomly. In this case the synchronization condition is fulfilled only for one of oscillatory modes.

**2.2. Experimental results: frequency adjustments.** Using anatomical criteria, neighboring nephrons having a high likelihood of deriving their afferent arterioles from the same interlobular artery were identified [19]. In these nephrons 29 out of 33 pairs (i.e., 80 %) were found to have synchronized oscillations. In contrast, nephron pairs not fulfilling these criteria only showed synchronous oscillations in one case out of 23 investigated pairs (i.e., 4 %). This observation shows that synchronized oscillations are preferentially found in nephrons originating from the same interlobular artery. Figure 7 displays the tubular pressure variations in pairs of neighboring nephrons for a normotensive rat (a) and for hypertensive rats (b-d). The oscillations presented in Figs.7 (b,c and d) are significantly more irregular than the oscillations displayed in (a). One can visually observe a certain degree of synchronization between the interacting nephrons. It is difficult, though, to separately estimate the degree of adjustment for the myogenic oscillations and for the TGF mediated oscillations without special tools.

To study interactive dynamics in coupled systems the newly developed wavelet based coherence measures can be successfully used [20]. In the present paper, we modify the approach proposed by Lachaux *et al.* [20] and introduce a coherence measure that is more appropriate for the purpose of our analysis. Fig. 8 shows two examples where the slow oscillations remain quite stationary while the frequencies of the fast oscillations vary significantly with time (they may be non-synchronous similar to Fig.8a, *but they may be also synchronous for neighboring nephrons!* - see Fig.8b). To analyze such situations we introduce a formalism where we can adjust the control frequency of the wavelet function rather than assuming some fixed value defined a priori [22]. This approach resembles to well-known sliding window analysis [21]. However, within the framework of the wavelet technique the window size is varied depending on the frequency: We need a small window to study high-frequency changes of the time series with good precision and a large window to study low-frequency spectral information. To examine entrainment phenomena between two rhythms in coupled biological oscillators (e.g., between the slow TGF-mediated motions or between the fast motions in neighboring nephrons) we have to follow the temporal evolution of rhythmic components (i.e., maxima of local spectra associated with these modes) and their coherence. Because such peaks (instantaneous frequencies of rhythmic components) may show large fluctuations relative to the

mean value, we consider a coherence measure for two interacting modes that depends on both time and frequency.

Let  $E_{xx}(f, t)$  and  $E_{yy}(f, t)$  be the energy densities of signals  $x(t)$  and  $y(t)$ . Let also in some range of frequencies  $\Delta$  each of the processes  $x(t)$  and  $y(t)$  has a clearly expressed rhythm (e.g., range of slow or fast oscillations for the two nephrons). In this case synchronization means that the corresponding frequencies for  $x(t)$  and  $y(t)$  will be locked (coincide). Such a situation corresponds to the value  $\Gamma_{\Delta} = 1$  for the function:

$$\Gamma_{\Delta}^2(t) = \frac{\max_{f \in \Delta} [E_{xy}(f, t)]^2}{\max_{f \in \Delta} [E_{xx}(f, t)] \cdot \max_{f \in \Delta} [E_{yy}(f, t)]}. \quad (9)$$

Here,  $E_{xy}(f, t)$  is the mutual energy density  $E_{xy}(f, t) = |T_{xy}(f, t) \cdot T_{yx}^*(f, t)|$ .  $\Gamma_{\Delta}(t)$  is a function of time that allows us to follow the evolution of the interactive dynamics of the two processes in the chosen frequency range  $\Delta$ . The more synchronous the rhythms of these processes are the closer  $\Gamma_{\Delta}(t)$  will be to 1.

In general when two frequencies are coincide we can speak about the property of coherence. To prove the presence of synchronization the phenomenon of phase or frequency locking should be studied. The advantage of nonstationary dynamics consists in the following. Because the frequency associated to one rhythm changes in time, using wavelets we can clearly see whether the second frequency follow these changes or not. That is why we can speak about the synchronization phenomena besides the coherence properties.

Figures 9 and 10 demonstrate different degrees of coherence for the considered modes. For periodic oscillations (Fig.9a and Fig.10a), both the slow and fast modes of the interacting nephrons are perfectly locked during the observation time. For a system with complex oscillations subjected to noise one can speak about a certain degree of synchronization if the periods of locking are large compared with the characteristic periods of oscillations [23]. Fully incoherent behavior with respect to both oscillatory modes can be observed in Fig.9b and Fig.10b. In many cases we can diagnose synchronization of the slow motions (Fig.9c,d) for relatively long time intervals where the frequencies remain almost equal. The fast motions, on the other hand, can demonstrate different coherence properties between nephrons. The oscillations can be locked during long periods of time together with the slow oscillations (Fig.10c). We define this type of synchronization as full synchronization since all time scales of the system are locked. Another case, illustrated in Figs.9d and 10d, is when the fast oscillations are incoherent while the slow oscillations are synchronized during the considered time interval. We refer to this phenomenon as partial synchronization.

**2.3. Experimental results: phase entrainments.** As discussed above neighboring nephrons influence each other's blood supply either through electrical signals that activate the vascular smooth muscle cells or through a hemodynamic coupling. The two mechanisms depend very differently on the precise structure of the arteriolar network. Hence, variations of this structure may determine which of the mechanisms is the more important. This could be of considerable biological interest, because the effects produced by the two mechanisms tend to be shifted in phase, and their influence on the overall behavior of the nephron system may be very different.

In an earlier paper [8], we studied phase relations between two signals using a Hilbert transformation. This approach works perfectly as long as we are not interested in the separated dynamics of different rhythmic activities in the oscillatory process. In our case, the multimode process has one dominant rhythm while the other rhythm is small in amplitude. To account

for this situation we introduce phases via wavelet-transform coefficients:

$$T_x(f, t) = |T_x(f, t)| \cdot \exp[i\varphi_x(f, t)], \quad (10)$$

where the phase function  $\varphi_x(f, t)$  depends on the considered mode. As it was discussed in [18, 20], we can calculate the wavelet coefficients for the chosen central frequency  $f_0$  of the wavelet function. The corresponding phases  $\varphi_x(f_0, t)$  are closely related to the phases introduced via Hilbert transform of the band-pass filtered signal [18]. An approach of band-pass filtration with the further definition of instantaneous phase was successfully used in [21]. The process of filtration can cause some technical problems in the case of nonstationary dynamics especially if two modes are close enough in the frequency domain. Such problems can be solved using sliding window analysis [21] or, alternatively, different aspects of multimode phase dynamics can be studied with wavelets.

In general, as a result of wavelet transform we obtain two-dimensional arrays of modulus  $|T_x(f, t)|$  and phases  $\varphi_x(f, t)$ . The latter means that the notion of phase is defined for each frequency  $f$  at any fixed time moment  $t$ . When considering two processes  $x(t)$  and  $y(t)$  the wavelet transform allows us to calculate the phase differences  $\varphi_x(f, t) - \varphi_y(f, t)$  and various synchronization factors [18]. In the case of clearly expressed rhythmic dynamics we don't need to know the complete two-dimensional phase spectrum  $\varphi_x(f, t)$  because we are interesting only in phases related to the rhythmic contributions. In the case when instantaneous frequencies of modes demonstrate large fluctuations relative to the mean value (similar to Fig.8), it seems to be useful adjust the central frequency of wavelet function according to these fluctuations. Hence, in this work we shall follow the time evolution of each mode in the frequency domain and at fixed moments of time  $t_0$  extract the phases related to the local peaks of the power spectrum  $E_x(f, t_0)$  (or  $|T_x(f, t_0)|$ ). For coupled nephrons this allows us to introduce phases for the slow and fast dynamics separately. To study synchronization phenomena in bivariate data it is possible to calculate the phase difference or the distribution of the cyclic relative phase [21].

Figure 11 shows an example of the (normalized) phase difference for the regular pressure variations in a normotensive rat. One clearly observes in-phase ( $\Delta\varphi \approx 0$ ) synchronization for fast mode and anti-phase ( $\Delta\varphi \approx \pi$ ) synchronization for slow oscillations in nephrons branching from different arterioles. Note, that fast oscillation in our analysis were always locked in phase, but there may be characteristic phase slips of  $2\pi k$  because of the noisy conditions under which the nephrons operate. The case of anti-phase synchronization for slow mode occurred rather seldom. More typical situation was when both, the slow and fast oscillations were synchronized in-phase. (This situation takes place for nephrons branching from the same arteriole).

Let us consider now how our phase approach is applied to chaotic dynamics as one typically observes for hypertensive rats. Figure 12 illustrates examples of phase dynamics for time series presented in Figure 7b,c. The phase differences indicate synchronous dynamics in Fig.12a and nonsynchronous in Fig.12b. The results for phase entrainment correspond to the results for frequency adjustments. In the case of synchronization for hypertensive rats we observed for all experimental data the in-phase regime ( $\Delta\varphi \approx 0$ ).

## Conclusions

Based on the analysis of experimental results we showed that the vascular dynamics and the tubuloglomerular feedback mechanism are responsible for two time scales associated with a fast and a slow oscillatory mode in the individual nephron. Both for periodic oscillations



observed in normotensive rats and for the chaotic oscillations in hypertensive rats the two modes exhibit resonant behavior as well as nonsynchronous dynamics.

To investigate different types of internephron mode entrainment we developed an approach based on a mutual wavelet transformation that allows us to easily analyze frequency and phase adjustments between different time scales from nonstationary data. We observed simultaneous (full) locking for the slow and fast oscillations both for normotensive and for hypertensive rats. We also identified a state of partial synchronization where the slow oscillations are synchronized while the fast motion demonstrates noncoherent behavior. Such a situation is typical for hypertensive rats.

Numerical simulations for coupled nephron models demonstrate similar behavior. With varying time delay in the tubuloglomerular feedback and varying strength of the vascular coupling the experimentally observed forms of synchronous behavior were recovered.

**Acknowledgments.** A.P. acknowledges support from CRDF (grant Y1-P-06-06). This work was also partly supported by INTAS grant (01-2061) and RFBR (01-02-16709).

## References

- [1] W. B. Cannon. Organization for physiological homeostasis // *Physiol. Rev.* 1929. Vol. 9. P. 399.
- [2] C. Nicolis and I. Prigogine. *Self-Organization in Nonequilibrium Systems*. Wiley, New York, 1977.
- [3] L. Glass and M.C. Mackey. *From Clocks to Chaos: The Rhythms of Life*. Princeton University Press, Princeton, 1988.
- [4] N.-H. Holstein-Rathlou, A.W. Wagner and D.J. Marsh. Tubuloglomerular feedback dynamics and renal blood flow autoregulation in rats // *Am. J. Physiol.* 1991. Vol. 260. P. F53; K.H. Chou, Yu-Ming Chen, V.Z. Mardarelis, D.J. Marsh and N.-H. Holstein-Rathlou. Detection of interaction between myogenic and TGF mechanisms using nonlinear analysis // *Am. J. Physiol.* 1994. Vol. 267. P. F160; R. Feldberg, M. Colding-Jorgensen and N.-H. Holstein-Rathlou. Analysis of interaction between TGF and the myogenic response in renal blood flow autoregulation // *Am. J. Physiol.* 1995. Vol. 269. P. F581.
- [5] N.-H. Holstein-Rathlou and P.P. Leyssac. TGF-mediated oscillations in the proximal intratubular pressure: Differences between spontaneously hypertensive rats and Wistar-Kyoto rats // *Acta Physiol. Scand.* 1986. Vol. 126. P. 333.
- [6] P.P. Leyssac and N.-H. Holstein-Rathlou. Effects of various transport inhibitors on oscillating TGF pressure response in the rat // *Pflügers Archiv.* 1986. Vol. 407. P. 285.
- [7] N.-H. Holstein-Rathlou and D.J. Marsh. Renal blood flow regulation and arterial pressure fluctuations: A case study in nonlinear dynamics // *Physiol. Rev.* 1994. Vol. 74. P. 637.
- [8] N.-H. Holstein-Rathlou, K.-P. Yip, O.V. Sosnovtseva and E. Mosekilde. Synchronization phenomena in nephron-nephron interaction // *Chaos.* 2001. Vol. 11. P. 417.
- [9] D.E. Postnov, O.V. Sosnovtseva, E. Mosekilde and N.-H. Holstein-Rathlou. Cooperative phase dynamics in coupled nephrons // *Int. J. Modern Physics B.* 2001. Vol. 15. P. 3079.
- [10] F. Mormann, K. Lehnertz, P. David, and C.E. Elger. Mean phase coherence as a measure of phase synchronization and its application to the EEG of epileptic patients // *Physica D.* 2000. Vol. 144. P. 358.

- [11] X.-J. Wang. Multiple dynamical modes of thalamic relay neurons: Rhythmic bursting and intermittent phase-locking // *Neuroscience*. 1994. Vol. 59. P. 21.
- [12] A. Neiman and D.F. Russell. Stochastic biperiodic oscillations in the electroreceptors of paddlefish // *Phys. Rev. Lett.* 2001. Vol. 86. P. 3443.
- [13] K.S. Jensen, E. Mosekilde and N.-H. Holstein-Rathlou. Selsustained oscillations and chaotic behaviour in kidney pressure regulation // *Mondes Develop.* 1986. Vol. 54/55. P. 91; N.-H. Holstein-Rathlou and D.J. Marsh. A dynamic model of the tubuloglomerular feedback mechanism // *Am. J. Physiol.* 1990. Vol. 258. P. F1448; N.-H. Holstein-Rathlou and D.J. Marsh. A dynamic model of renal blood flow autoregulation // *Bull. Math. Biol.* 1994. Vol. 56. P. 441.
- [14] E. Mosekilde. *Topics in Nonlinear Dynamics: Applications to Physics, Biology and Economic Systems*. World Scientific, Singapore, 1996; M. Barfred, E. Mosekilde, and N.-H. Holstein-Rathlou. Bifurcation analysis of nephron pressure and flow regulation // *Chaos*. 1996. Vol. 6. P. 280.
- [15] M.D. Andersen, N. Carlson, E. Mosekilde and N.-H. Holstein-Rathlou, Dynamic model of nephron-nephron interaction // in *Membrane Transport and Renal Physiology*, H. Layton and A. Weinstein (eds) (Springer-Verlag, New York, 2001).
- [16] P.P. Leyssac and N.-H. Holstein-Rathlou. Tubulo-glomerular feedback response: Enhancement in adult spontaneously hypertensive rats and effects of anaesthetics // *Pflügers Arch.* 1989. Vol. 413. P. 267.
- [17] A. Grossmann, J. Morlet. Decomposition of hardy functions into square integrable wavelets of constant shape // *S.I.A.M. J. Math. Anal.* 1984. Vol. 15. P. 723; I. Daubechies. *Ten Lectures on Wavelets*. S.I.A.M., Philadelphia, 1992; P.Ch. Ivanov, L.A.N. Amaral, A.L. Goldberger, S. Havlin, M.G. Rosenblum, Z. R. Struzik, H.E. Stanley. Multifractality in human heartbeat dynamics // *Nature*. 1999. Vol. 399. P. 461.
- [18] R.Q. Quiroga, A. Kraskov, T. Kreuz, P. Grassberger. Performance of different synchronization measures in real data: A case study on electroencephalographic signals // *Phys. Rev. E*. 2002. Vol. 65. P. 041903.
- [19] Y.-M. Chen, K.-P. Yip, D.J. Marsh, and N.-H. Holstein-Rathlou. Magnitude of TGF-initiated nephron-nephron interactions is increased in SHR // *Am. J. Physiol.* 1995. Vol. 269. P. F198.
- [20] J.P. Lachaux, E. Rodriguez, M. Le Van Quyen, A. Lutz, J. Martinerie, F.J. Varela. Studying single-trials of phase synchronous activity in the brain // *Int.J. Bifurcation Chaos*. 2000. Vol. 10. P. 2429.
- [21] P. Tass, M.G. Rosenblum, J. Weule, J. Kurths, A. Pikovsky, J. Volkman, A. Schnitzler, H.-J. Freund. Detection of n:m phase locking from noisy data: application to magnetoencephalography // *Phys. Rev. Lett.* 1998. Vol. 81. P. 3291.
- [22] O.V. Sosnovtseva, A.N. Pavlov, E. Mosekilde, N.-H. Holstein-Rathlou. Bimodal oscillations in nephron autoregulation // *Phys. Rev. E*. 2002. Vol. 66. P. 061909.
- [23] L.R. Stratonovich. *Topics in the Theory of Random Noise*. Gordon and Breach, New York, 1963.

*Physics Department,  
Saratov State University, Russia  
Department of Physics,  
Technical University of Denmark  
Department of Medical Physiology,  
Panum Institute,  
University of Copenhagen, Denmark*

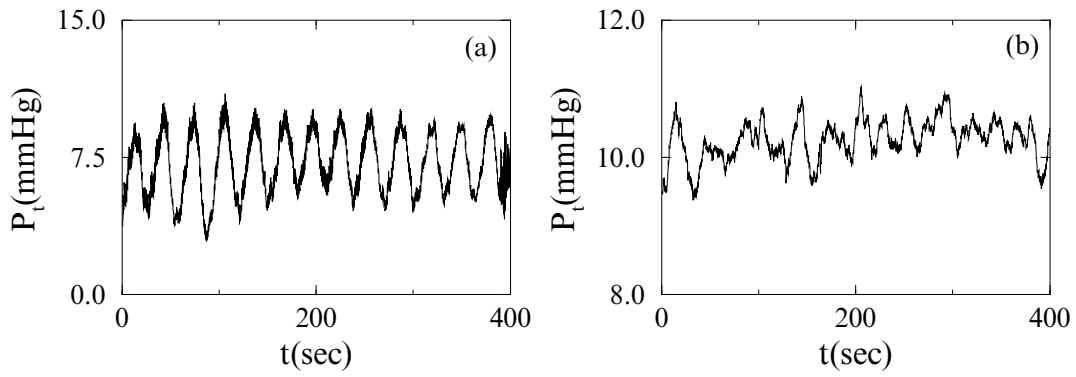


Figure 1: Regular tubular pressure oscillations from a normotensive rat (a) and irregular pressure variations from a spontaneously hypertensive rat (b).

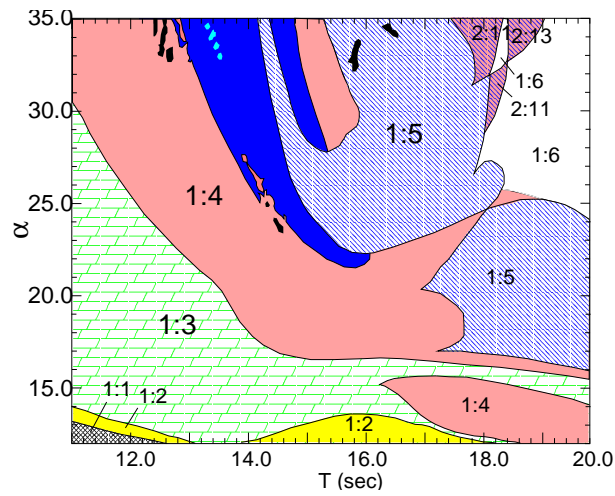


Figure 2: Two-mode oscillatory behavior in the single nephron model. Black colored regions correspond to a chaotic solution.

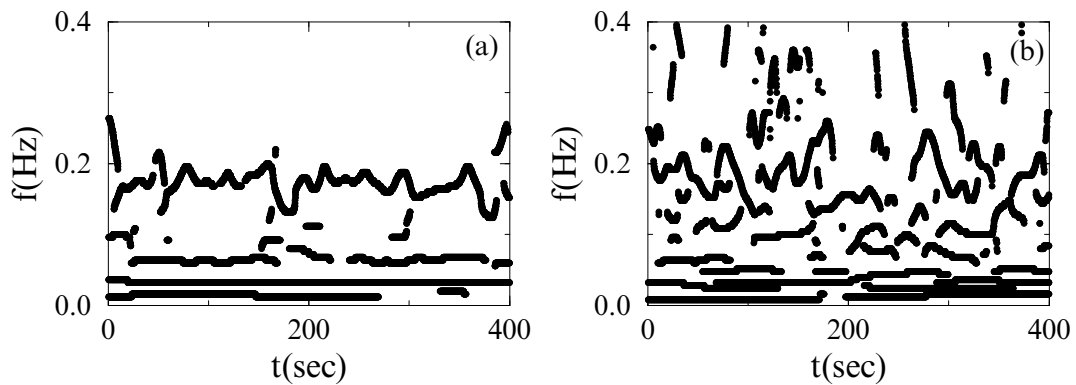


Figure 3: Wavelet analysis of the two time-series presented in Fig.1.

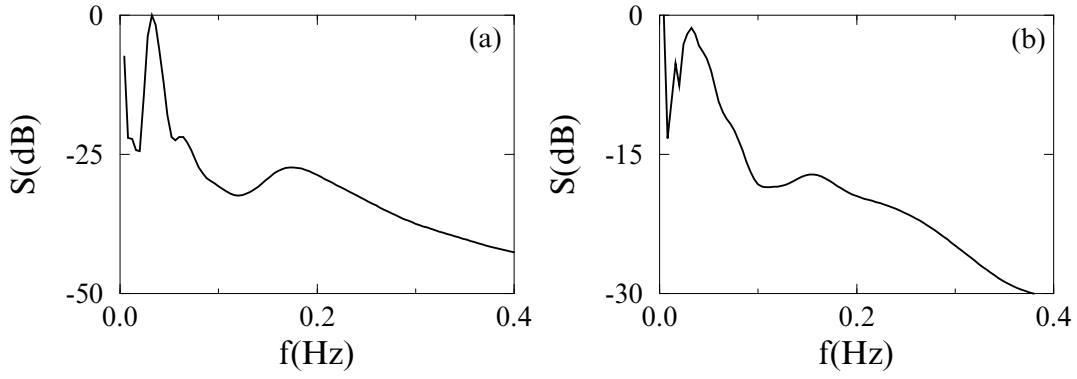


Figure 4: Power spectrum obtained from the wavelet analysis for the two time-series presented in Fig.1. Two peaks, representing the fast myogenic oscillations and the slower tubuloglomerular oscillations, are well-distinguished.

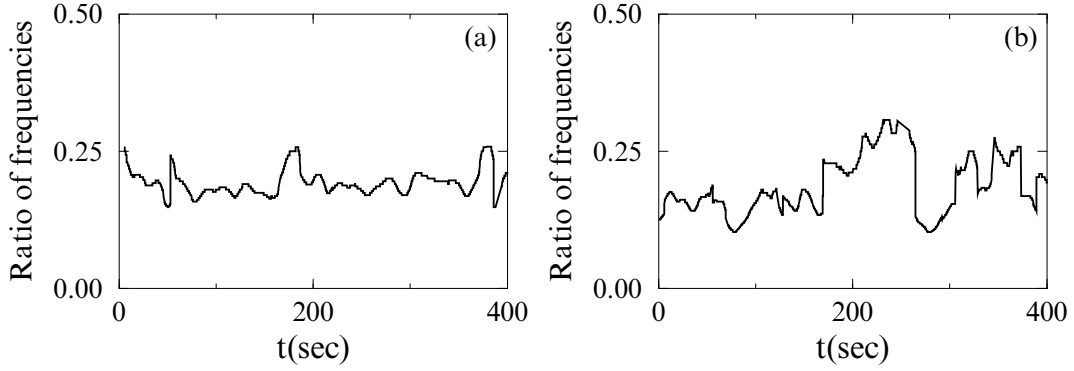


Figure 5: Ratio of the internal time-scales for a normotensive rat (a) and for a hypertensive rat (b).

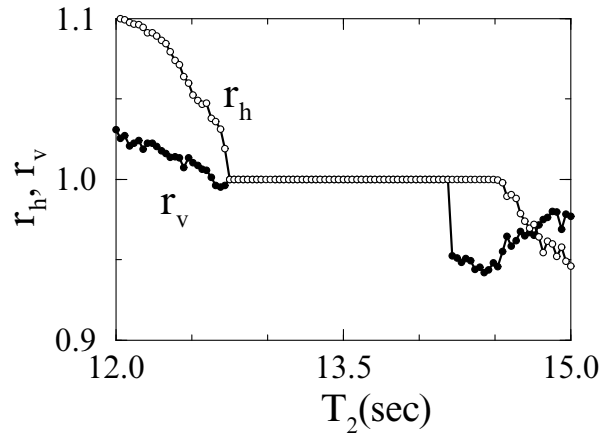


Figure 6: Full and partial synchronization of fast and slow motions ( $T_1 = 13.5 \text{ sec}$ ,  $\alpha = 30.0$  and  $\gamma = 0.06$ ).

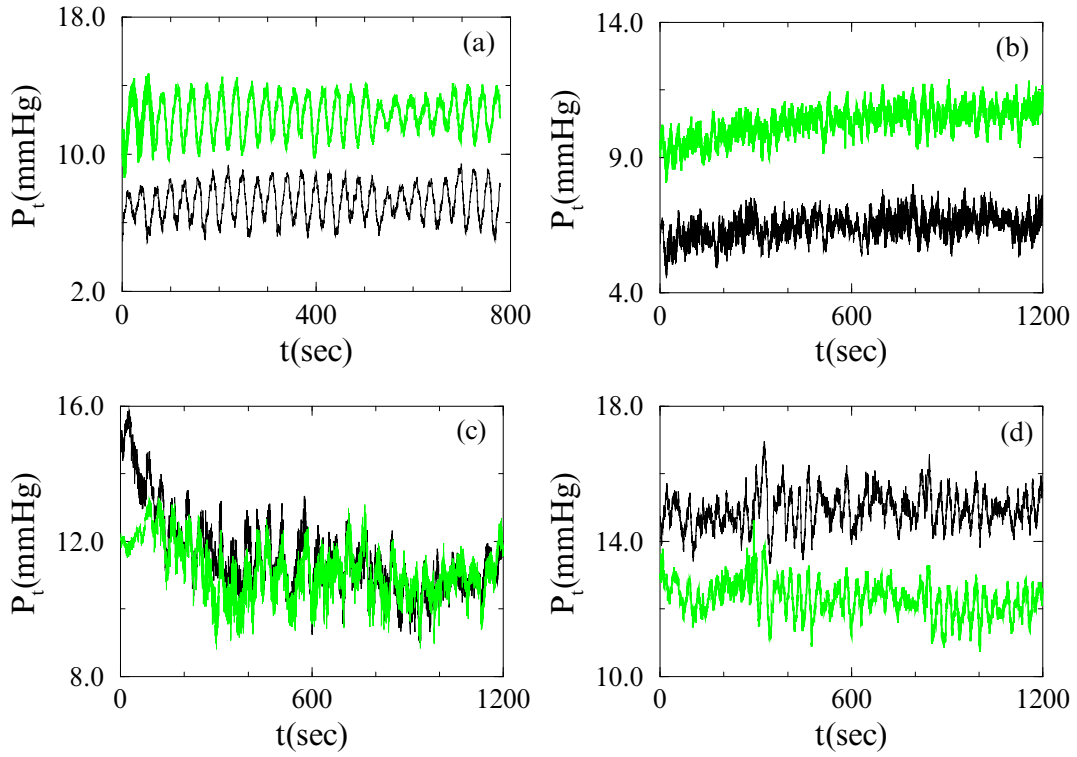


Figure 7: Examples of the tubular pressure variation that one can observe in adjacent nephrons (a) for normotensive and (b-d) for hypertensive rats.

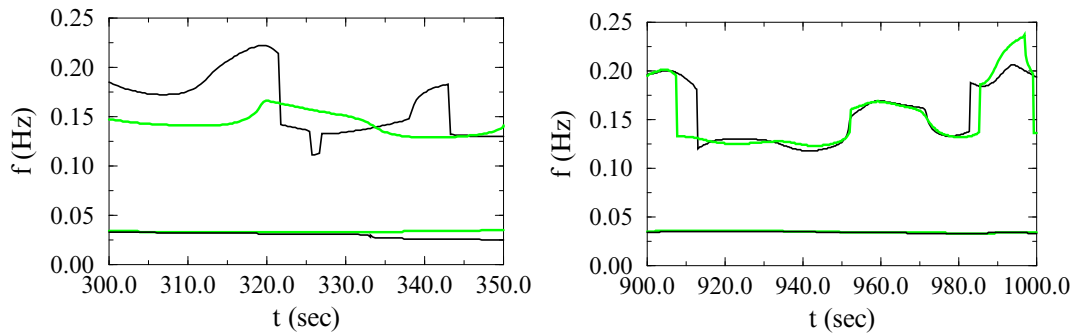


Figure 8: Examples of nonstationary non-synchronous (a) and nonstationary synchronous (b) dynamics of the fast oscillatory modes. In both cases slow modes demonstrate stationary synchronous state.

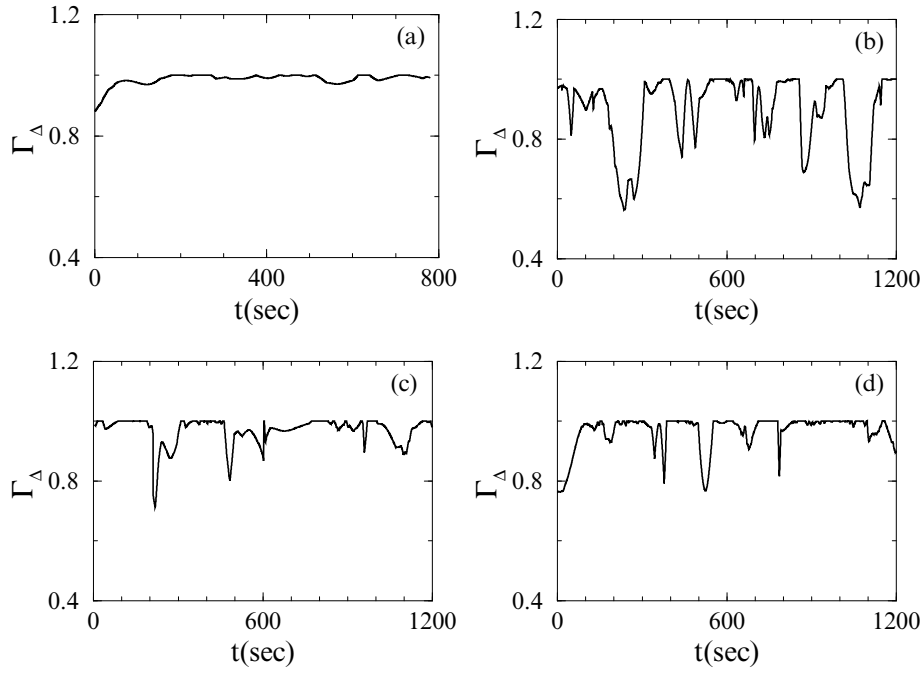


Figure 9: Mutual wavelet analysis for the slow oscillations of the two time-series presented in Fig.7: (a) synchronous behavior, (b) nonsynchronous dynamics, (c) and (d) synchronous behavior but during limited time intervals.

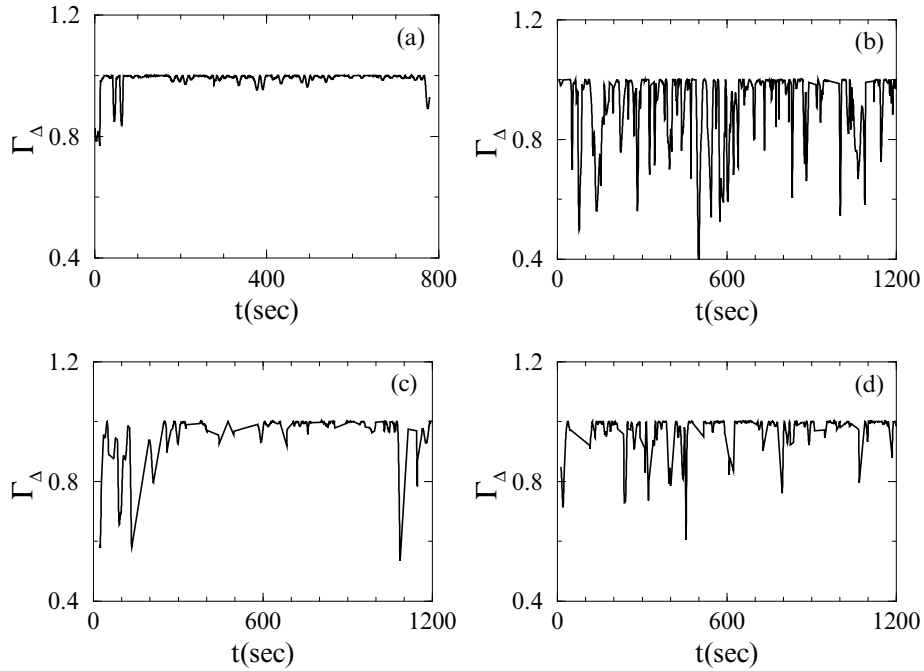


Figure 10: Mutual wavelet analysis for the fast oscillations extracted from time-series presented in Fig.7. (a) and (c) illustrate synchronous behavior, (b) and (d) nonsynchronous dynamics.

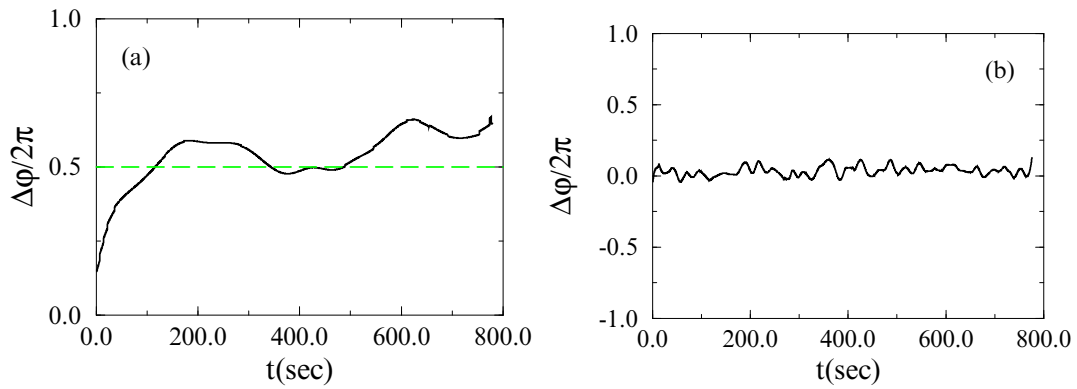


Figure 11: Phase differences for the slow (a) and fast (b) oscillations of the coupled nephrons. The given results are obtained for the time series presented in Fig.7a (normotensive rat).

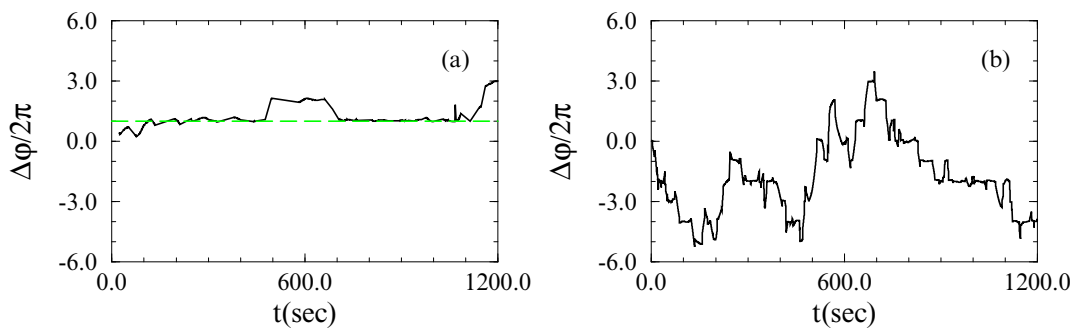


Figure 12: Phase differences for the fast synchronous (a) and for the fast non-synchronous dynamics (b). The given examples are obtained for the time series of hypertensive rats shown in Fig.7 (c and b, respectively).